

---

Proceedings of the National Conference on Neutron Scattering and the Complementary Methods in the Investigations of the Condensed Phases, Chlewska 2007

## Magnetic Structure of RCuIn (R = Nd, Tb, Ho, Er)

A. SZYTUŁA<sup>a</sup>, A. ARULRAJ<sup>b</sup>, S. BARAN<sup>a</sup>, T. JAWORSKA-GOŁĄB<sup>a</sup>,  
B. PENC<sup>a</sup>, N. STÜSSER<sup>b</sup>, YU. TYVANCHUK<sup>c</sup> AND A. ZARZYCKI<sup>a</sup>

<sup>a</sup>M. Smoluchowski Institute of Physics, Jagiellonian University  
Reymonta 4, 30-059 Kraków, Poland

<sup>b</sup>BENSC, Hahn–Meitner Institute

Berlin-Wannsee, Glienicke Str. 100, D-14-109 Berlin, Germany

<sup>c</sup>Department of Inorganic Chemistry, Ivan Franko National University of Lviv  
Kyryla and Mefodiya 6, UA-79005 Lviv, Ukraine

*Dedicated to Professor Jerzy Janik on the occasion of his 80th birthday*

Magnetic and neutron diffraction measurements of RCuIn (R = Nd, Tb, Ho, Er) are reported. The compounds crystallize in the hexagonal ZrNiAl-type structure. The ZrNiAl lattice originates from a distortion of a kagomé lattice. The studied compounds are antiferromagnets with the Néel temperature equal to 4.9 K for R = Nd, 14.5 K for R = Tb, 4.5 K for R = Ho and 3.5 K for R = Er. The magnetic ordering is described by the propagation vector  $\mathbf{k} = (1/2, 1/2, k_z)$  with  $k_z$  equal to 0.161(6) for R = Nd, 0.2213(5) for R = Tb, 0.2510(3) for R = Ho and 0 for R = Er. The magnetic structure is noncollinear with magnetic moments in the basal plane for R = Nd, Tb and Ho and collinear with magnetic moments parallel to the  $c$ -axis for R = Er. The observed magnetic ordering results from the competition between exchange interactions of the Ruderman–Kittel–Kasuya–Yosida type, the geometrical frustration of the rare-earth magnetic moments and the influence of the crystal electric field. The latter affects the direction of magnetic moments and is responsible for the magnetic crystalline anisotropy.

PACS numbers: 61.12–q, 71.20.Lp, 75.25.+z, 75.50.Ee

### 1. Introduction

RTX ternary compounds (R = rare earth, T =  $d$ -electron metal, X =  $p$ -electron element) crystallize in hexagonal structures of the ZrNiAl-type (Fig. 1) and exhibit intriguing physical properties, which are often governed by geometrical frustration within the R-sublattice (triangular coordination). In case of antiferromagnetic interactions, geometrical frustration of rare-earth magnetic moments

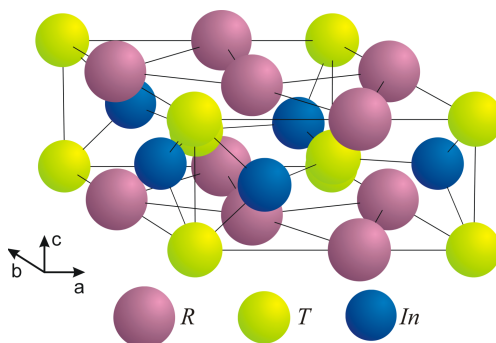


Fig. 1. Crystal unit cell of the RTIn compounds (ZrNiAl-type).

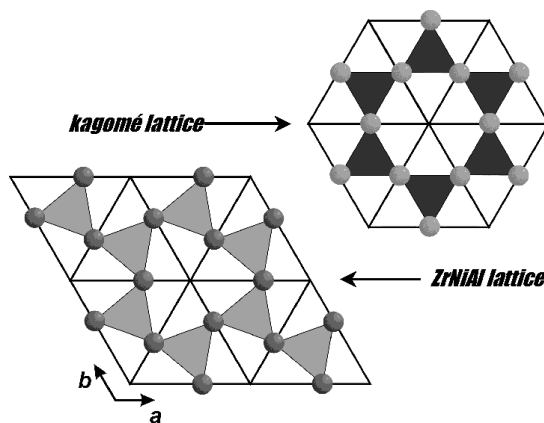


Fig. 2. Distribution of the rare-earth atoms in  $a$ - $a$  plane of ZrNiAl-type structure and comparison with the kagomé lattice.

(Fig. 2) leads to a complex magnetic phase diagram in triangularly arranged lattices [1].

For the RCuIn series magnetic properties were investigated only for R = Ce, Gd and Tb. CeCuIn is a paramagnet down to 4.2 K [2]. GdCuIn orders antiferromagnetically below  $T_N = 20$  K [3] while the magnetic data for TbCuIn exhibit two maxima at 16 and 84 K in the temperature dependence of magnetic susceptibility [4].

Neutron diffraction data for TbCuIn collected in the temperature range 1.5 K and 50 K confirm the hexagonal crystal structure at 50 K. At 1.5 K the Tb magnetic moments form a noncollinear magnetic structure described by the propagation vector  $\mathbf{k} = (1/2, 1/2, 0.2288(3))$  [4].

This work presents magnetic and neutron diffraction data for RCuIn (R = Nd, Tb, Ho, and Er) compounds. From the data the magnetic structures of these compounds have been determined.

## 2. Experimental details

Polycrystalline samples were prepared by arc melting of high-purity raw metals (rare earths with purity not worse than 99.8 wt.% main component, electrolytic copper with purity 99.92 wt.% Cu, and indium with purity 99.99 wt.% In) in titanium gettered argon atmosphere ( $P = 50$  kPa). The total mass of each ingot was about 7 g. The weight losses during preparation did not exceed 1 wt.%. All prepared alloys were annealed at 870 K for 100 h in evacuated silica tubes and then quenched in cold water.

X-ray powder diffraction patterns were recorded at room temperature using Cu  $K_\alpha$  radiation with a Philips X'PERT type diffractometer. DC magnetic measurements were carried out using a commercial MPMS SQUID magnetometer in the temperature range  $2 \div 300$  K in magnetic fields up to 50 kOe. The E6 diffractometer at the Berlin Neutron Scattering Center was used to carry out diffraction measurements in the temperature range 1.5 and 50 K with the incident neutron wavelength 2.444 Å. The neutron diffraction data were analyzed using the Rietveld-type program Fullprof [5].

## 3. Results

A typical X-ray diffraction pattern for HoCuIn is shown in Fig. 3. The X-ray at room temperature and the neutron diffraction data at low temperatures in paramagnetic state (Fig. 4) confirm that all RCuIn compounds have the hexagonal ZrNiAl type structure with the following position of atoms in the crystal unit cell: R atoms at the 3(g) site:  $x_R, 0, 1/2$ ; Cu atoms at the 1(b) site:  $0, 0, 1/2$  and 2(c) site:  $1/3, 2/3, 0$ ; and In atoms at the 3(f) site:  $x_{In}, 0, 0$ . The determined lattice parameters and  $x_i$  parameters are listed in Table I.

TABLE I

Crystal structure parameters of RCuIn ( $R = Nd, Tb, Ho, Er$ ).

	NdCuIn		TbCuIn		HoCuIn		ErCuIn	
	300	8	300	10	300	10	300	25
$T$ [K]	300	8	300	10	300	10	300	25
$a$ [Å]	7.4715 (3)	7.4485 (13)	7.4585 (5)	7.4276 (12)	7.4299 (6)	7.4147 (8)	7.4186 (4)	7.4012 (10)
$c$ [Å]	4.1668 (2)	4.1459 (7)	3.9657 (3)	3.9032 (11)	3.9058 (4)	3.8843 (6)	3.8890 (3)	3.8571 (7)
$V$ [Å <sup>3</sup> ]	201.437 (25)	199.193 (103)	191.05 (4)	186.48 (11)	186.72 (4)	184.93 (70)	185.26 (3)	182.97 (8)
$x_R$	0.5869 (3)	0.5869 (8)	0.5900 (5)	0.5927 (9)	0.5934 (6)	0.5912 (9)	0.5894 (5)	0.5892 (9)
$x_{In}$	0.2470 (4)	0.2465 (17)	0.2500 (6)	0.2478 (23)	0.2542 (6)	0.2526 (20)	0.2555 (5)	0.2502 (19)
$R_{\text{prof}}$	9.7%	8.7%	7.8%	4.3%	6.9%	4.5%	6.8%	4.4%
$R_{\text{Bragg}}$	8.3%	7.0%	7.5%	3.8%	6.6%	5.9%	5.9%	3.5%

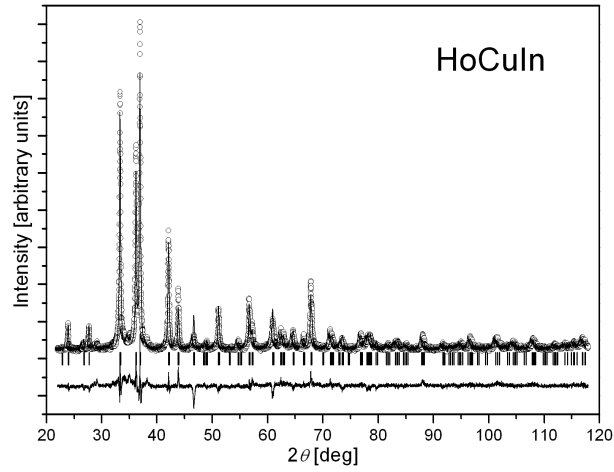


Fig. 3. X-ray diffraction pattern of powder HoCuIn at room temperature. The circles represent experimental points, the solid lines are the calculated profile and the difference between the observed and the calculated intensity (the bottom of each diagram). The vertical bars indicate the positions of the Bragg peaks.

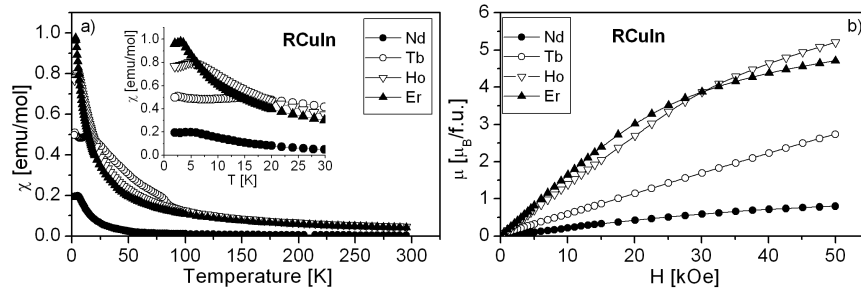


Fig. 4. (a) Temperature dependence of the magnetic susceptibility (inset shows the low temperature parts) and (b) the magnetization curve at 2 K for RCuIn ( $R = \text{Nd, Tb, Ho, Er}$ ) compounds.

Results of the magnetic measurements are presented in Fig. 4. These results indicate that the Néel temperature is 4.9 K for  $R = \text{Nd}$ , 14.5 K for  $R = \text{Tb}$ , 5.0 K for  $R = \text{Ho}$ , and 3.5 K for  $R = \text{Er}$ . In the paramagnetic phase the reciprocal magnetic susceptibility obeys the Curie–Weiss law with the negative value of the paramagnetic Curie temperature and the effective magnetic moment close to the free  $R^{3+}$  ion value. Values of the magnetic moments at  $T = 2$  K and the magnetic field  $H = 50$  kOe are smaller than the appropriate free  $R^{3+}$  ion values. The results of the magnetic measurements are summarized in Table II.

Typical neutron diffraction pattern for HoCuIn and ErCuIn is presented in Fig. 5. At 1.5 K the additional peaks due to a magnetic ordering are observed. An

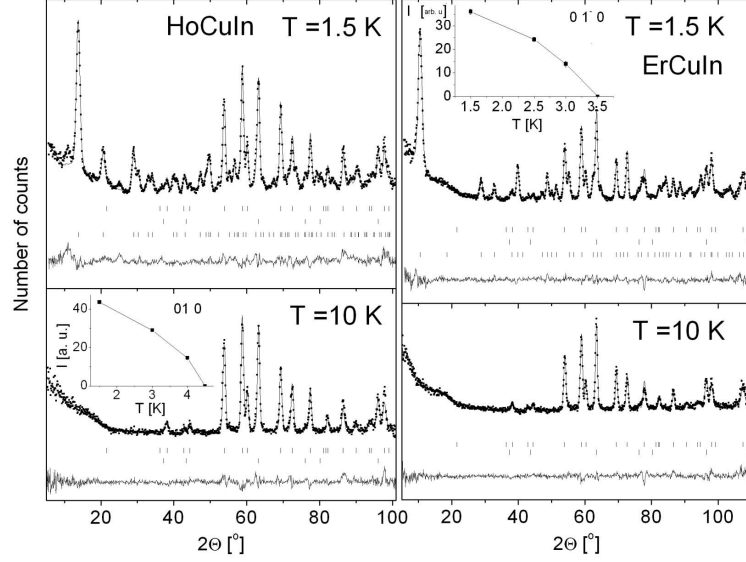


Fig. 5. Neutron diffraction patterns of HoCuIn and ErCuIn compounds collected at 1.5 and 10 K. The squares represent experimental points, the solid lines are the calculated profiles for the crystal and magnetic structure models (as described in the text) and the difference between the observed and the calculated intensity (the bottom of each diagram). The vertical bars indicate the positions of the Bragg peaks of nuclear and magnetic origin, respectively. The insets show the temperature dependence of the magnetic peak intensity.

TABLE II

Magnetic data for  $RCuIn$  ( $R = Tb, Ho, Er$ ).

R	$T_N$ [K]	$\theta_p$ [K]	$\mu_{\text{eff}}$ [ $\mu_B$ ]		$\mu_{\text{eff}}$ [ $\mu_B$ ]			
			exp.	theor.	exp. $M^*$	exp. $ND^{**}$	theor.	
Nd	4.9	-7.2	2.40	3.58	0.7	1.28(15)		3.2
Tb	14.5	-5.4	9.44	9.72	2.7	6.3(1)	6.0(4)	9.0
Ho	5.0	-10.0	10.51	10.65	5.2	8.6(2)	6.2(4)	10.0
Er	3.1	-12.3	9.93	9.65	4.7	7.1(1)	2.1(4)	9.0

\*from magnetization measurements at  $T = 2$  K and  $H = 50$  kOe;\*\*from neutron diffraction measurements at  $T = 1.5$  K

analysis of these patterns at 1.5 K leads to the following model of the magnetic structures:

- a noncollinear structure described by the propagation vector  $\mathbf{k} = (1/2, 1/2, k_z)$  with  $k_z$  equal to 0.161(6) for NdCuIn, 0.2213(5) for TbCuIn and 0.2510(3) for HoCuIn,

— a collinear structure described by the propagation vector  $\mathbf{k} = (1/2, 1/2, 0)$  for ErCuIn.

In the ZrNiAl-type structure the R magnetic moments are located at positions:  $\mu_1(x_R, 0, 1/2)$ ,  $\mu_2(\bar{x}_R, \bar{x}_R, 1/2)$  and  $\mu_3(0, x_R, 1/2)$ . In NdCuIn all three Nd moments equal to  $1.29(15) \mu_B$  are parallel to each other and form the angle of  $\theta = 45^\circ$  with the  $c$ -axis and  $\varphi = 45^\circ$  with the  $a$ -axis. For TbCuIn the  $\mu_1$  and  $\mu_3$  moments, equal to  $6.3(2) \mu_B$ , are parallel and perpendicular to the  $a$ -axis while  $\mu_2$ , equal to  $6.0(4) \mu_B$ , is parallel to the [110] direction. In HoCuIn  $\mu_1$  and  $\mu_3$  equal to  $8.6(2) \mu_B$  are perpendicular for the  $a$ -axis while  $\mu_2$  equal to  $6.2(4) \mu_B$  forms angle  $34^\circ$  with the  $a$ -axis. In ErCuIn all Er moments are parallel to the  $c$ -axis and equal to  $7.1(1) \mu_B$  for  $\mu_1$  and  $\mu_3$  and to  $2.1(4) \mu_B$  for  $\mu_2$ .

Temperature dependence of the magnetic peak intensities gives an information on changes in the magnetic structure. For TbCuIn this dependence has a complex character. With increasing temperature the intensities of the Bragg peaks decrease whereas the intensities of the diffusion peaks increase. The intensities of the Bragg peaks decrease to zero at the Néel temperature equal to 14.5 K while diffusion peaks exist up to 24 K.

In HoCuIn intensities of the magnetic peaks decrease to zero at the Néel temperature equal to 4.5 K (see the inset in Fig. 5). Similar dependence for ErCuIn gives the Néel temperature equal to 3.5 K. The neutron diffraction results reported above are in good agreement with the magnetometric data.

#### 4. Discussion

The data presented in the work confirm that the RCuIn (R = Nd, Tb, Ho, and Er) compounds crystallize in the hexagonal ZrNiAl-type crystal structure and order antiferromagnetically at low temperatures. In the ZrNiAl-type crystal structure the rare-earth atoms are placed in the  $a$ - $b$  planes separated by non-magnetic Cu-In layers. This leads to conclusions that the magnetic structure of these compounds can be considered as having quasi-two-dimensional character. The magnetic ordering is described by the propagation vector  $\mathbf{k} = (1/2, 1/2, k_z)$ . The values of  $k_z$  and the direction of the magnetic moments change with increasing number of  $4f$  electrons. The rare-earth magnetic moments form a modulated structure commensurate with the crystal structure in the (001) plane and in all the compounds, except ErCuIn, an additional modulation along  $c$ -axis was also observed. The magnetic order in the (001) plane is connected with the crystal structure of these compounds. The rare-earth atoms in the basal plane form a distorted kagomé lattice. Triangular order of the rare-earth atoms frustrates the magnetic interactions leading to non-collinear magnetic structures. The complex planar magnetic structures of TbCuIn and HoCuIn result from the geometrical frustration of exchange interactions, including the Dzialoshinski-Moriya interaction.

An existence of the modulated magnetic structure along the  $c$ -axis indicates long-range interactions. The interaction between the magnetic (001) plane is probably of the Ruderman–Kittel–Kasuya–Yosida (RKKY) type. The interaction of the RKKY-type is proportional to the de Gennes function  $(g_J - 1)^2 J(J + 1)$ . The values of this function decrease with increasing number of  $4f$  electrons. The dependence of the  $T_N$  value on the de Gennes factor is shown in Fig. 6. The obtained results indicate that this relation is satisfied in  $RCuIn$  compounds.

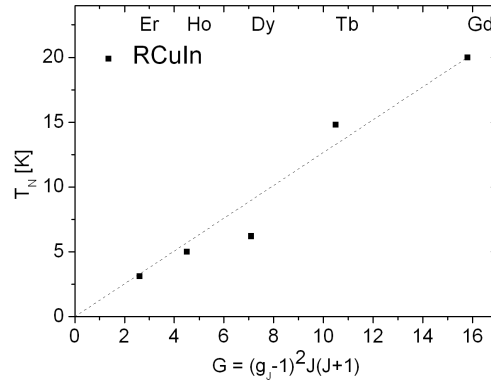


Fig. 6. The dependence of the Néel temperature as a de Gennes function for  $RCuIn$ . The data for  $R = Gd$  and  $Dy$  are from Ref. [8].

The second factor which influences the magnetic ordering is of the nature of the low-lying crystal field levels. The lowest-order term of the crystal field interaction is determined by the second-order Stevens factor  $\alpha_J$  which is negative for  $R = Tb, Dy, Ho$  and positive for  $R = Er$ . Inspection of our results indicates that for  $R = Tb$  and  $Ho$  the rare-earth magnetic moments lie in the basal plane while for  $R = Er$  they are parallel to the  $c$ -axis. This suggests that the crystal field interactions play a major role in determining the direction of the magnetic moment. The decrease in the values of the magnetic moments in the ordered state is also connected with the influence of the crystal electric field.

In  $TbCuIn$  complex magnetic properties are observed. Below the Néel temperature both, the short- and long-range order are observed. The short-range order exists above  $T_N$ . The existence of the short-range order above  $T_N$  was also observed in the isostructural  $TbAuIn$  [6]. Detailed investigations indicate that the cluster glass system exists in this compound above the Néel temperature [7].

## 5. Conclusions

Ternary  $RCuIn$  ( $R = Tb, Ho, Er$ ) compounds which order in the hexagonal  $ZrNiAl$ -type crystal structure order antiferromagnetically at low temperatures within the magnetic ordering scheme described by the propagation vector  $\mathbf{k} = (1/2, 1/2, k_z)$ . The values of  $k_z$  and direction of the magnetic moments change

with increasing number of  $4f$  electrons of the rare-earth elements. These suggest complex magnetic interactions between rare-earth magnetic moments including interaction via polarized conduction electrons (RKKY) and influence of the crystal electric field.

### Acknowledgments

This work was supported by the European Commission under the Sixth Framework Programme through the Key Action: Strengthening the European Research Area, Research Infrastructures Contract: H113-CT-203-505925 (NM13) and by Polish Ministry of Science and Information Society Technologies in Poland with grant No. 1 P03B 111 29. Three of the authors (S.B., B.P. and A.Sz.) would like to express their gratitude to the management of the BENSIC for financial support and kind hospitality. Yu.T. would like to acknowledge the financial support from Józef Mianowski Fund and kind hospitality of the Institute of Physics of the Jagiellonian University.

### References

- [1] H. Kawamura, *J. Phys., Condens. Matter.* **10**, 4707 (1998).
- [2] S.K. Malik, D.T. Adroja, B.D. Padalia, R. Vijavaghavan, *Physica B* **163**, 89 (1990).
- [3] J.W.C. de Vries, R.C. Thiel, K.H.J. Buschow, *J. Less-Common Metals* **111**, 313 (1985).
- [4] G. Ehlers, Ph.D. Thesis, Technische Universität Berlin, 1996.
- [5] J. Rodriguez-Carvajal, Program FullProf, Lab. Leon Brillouin, CEA-CNRS, 2000.
- [6] A. Szytuła, W. Bażela, Ł. Gondek, T. Jaworska-Gołąb, B. Penc, N. Stüsser, A. Zygmunt, *J. Alloys Comp.* **336**, 11 (2002).
- [7] Ł. Gondek, A. Szytuła, M. Bałanda, W. Warkocki, A. Szewczyk, M. Gutowska, *Solid State Commun.* **136**, 26 (2005).
- [8] A. Szytuła, Yu. Tyvanchuk, A. Zarzycki, T. Jaworska-Gołąb, Ya. Kalychak, in: *Proc. IX Int. Conf. on Crystal Chemistry of Intermetallic Compounds, Lviv 2005*, p. 130.